Steady Shear and Viscoelastic Properties of a Micro-Crosslinked Acrylamide-Based Terpolymer

Chuanrong Zhong, Xianghao Meng, Jun Deng

State Key Laboratory of Oil and Gas Reservoir Geology and Exploitation, Chengdu University of Technology, Chengdu 610059, Sichuan, China

ABSTRACT: A water-soluble micro-crosslinked associating polymer (PASA-PL): poly (acrylamide/butyl styrene/sodium 2-acrylamido-2-methylpropane sulphonate) (PASA)–phenolic aldehyde (PL) was prepared to reduce the critical associated concentration and enhance the thickening properties for the linear PASA polymer in aqueous and brine solutions. The consecutive steady shear and viscoelastic properties were investigated to explore the correlations between the rheologic performance and supramolecular structures for the PASA-PL brine solutions. Upon consecutive steady shear, the intermolecular hydrophobic association is greatly reinforced because of the expansion of the coiled PASA-PL chains at the suitable shear rate, and the brine solution exhibits obvious shear thickening behavior. The steady shear results show that the intermolecular hydrophobic association is reversible, and that the polymer chains do not degrade upon shearing. The PASA-PL brine solutions with 50 g L^{-1} NaCl have predominantly elastic character over the angular frequency range at the polymer concentration higher than 1.0 g L^{-1}, which is remarkably strengthened with a slight increase in polymer concentration. The PASA-PL brine solutions display a salt-thickening effect and predominantly exhibit elastic character over the angular frequency range at 10–50 g L^{-1} NaCl. These results demonstrate that the viscoelastic behavior of the PASA-PL solutions mainly depends on the formation of hydrophobically associated structures via the intermolecular association strengthened by the micro-crosslink of PASA with PL. © 2010 Wiley Periodicals, Inc. J Appl Polym Sci 120: 666–675, 2011

Key words: acrylamide micro-crosslink; hydrophobic association; viscoelastic properties; viscosity

INTRODUCTION

The fluidity ratio of injected aqueous phase to oil phase is generally higher than 1.0 in enhanced oil recovery (EOR). This results in a low sweep efficiency of aqueous phase. Therefore, a small amount of oil-flooding polymer is added to the aqueous phase fluid to increase remarkably the solution viscosity. As a result, the fluidity ratio of aqueous phase to oil phase can be reduced and the sweep efficiency of the aqueous phase is raised. The applied widely oil-flooding polymers are partially hydrolyzed polyacrylamide (HPAM) with the super-high molecular weight (1.0×10^7–2.8×10^7 g mol^{-1}) and modified acrylamide-based polymers. The HPAM polymer is conventionally micro-crosslinked with a small amount of organic trivalent aluminum, organic trivalent chromium, aldehydes, phenols, etc.[1–3] to enhance the heat and salt resistance and reduce the expended amount in the oil reservoirs with high-permeability. But the micro-crosslinked HPAM easily dehydrates in brine solutions and is likely to plug up the pore throats in the oil reservoirs because of the formation of the polymer gel with too high molecular weight. In the previous research work of our group, to obtain a polymer whose sizes of chains and solution properties are respectively accordant with the sizes of the pore throats and the expected properties of oil-flooding polymer applied in the high-permeability oil reservoirs with high salinity and temperature, A hydrophobically associating copolymer: poly [acrylamide (AM)/butyl styrene (BST)/sodium 2-acrylamido-2-methylpropane sulphonate (NaAMPS)] (PASA) with low molecular weight[4] was micro-crosslinked with a small amount of phenolic aldehyde (PL). Consequently, the micro-crosslinked PASA-PL polymer with excellent liquidity and water solubility was prepared. PASA-PL displays the excellent solution properties such as thickening and anti-ageing properties in brine solutions at a polymer concentration <1.5 g L^{-1}.[5]

The associating polymer aqueous solutions are non-Newtonian fluids. While flowing through smaller pore throats or larger pores in oil reservoirs, the polymer chains can be expanded upon shearing or coiled, and then the associated structures also change. Therefore, the polymer solutions display

elastic behavior as well as viscous behavior in the porous medium, which exhibited a viscoelastic effect. The viscoelastic properties of polymers are favorable for an increase in the microscopic oil-displacement efficiency in EOR, the residual oil in "dead ends" was pulled out by the viscoelastic polymer solution,[6] and the thickness of residual oil film reduces with increasing the elasticity of polymer solution.[7] Hence, the viscoelastic behavior of polymer solutions plays a significant role in enhancing oil recovery ratio. The viscoelastic behavior of linear hydrophobically associating acrylamide-based polymers and the influence factors have been reported by some literatures.[8,9] However, so far some deficiencies of these polymers have not yet been improved. For example, their critical associated concentrations (C_p^*) are on the high side in brine solutions, the apparent viscosities of brine solutions are low below C_p^* because of low molecular weights.[10] Few studies on micro-crosslinked associating acrylamide-based copolymers are investigated to enhance the solution properties of these linear polymers. The micro-crosslinked PASA-PL polymers with high apparent viscosities in brine solutions have been obtained.[5] To reveal the relationship between the intermolecular hydrophobic association and the apparent viscosities of the brine solutions for PASA-PL, in this article, the influence of micro-crosslink on thickening properties and the steady shear behavior were measured for the PASA-PL brine solution. Moreover, the viscoelastic properties of PASA-PL brine solutions were investigated as a function of polymer concentration, NaCl concentration and hydrophobic monomer feed amount to explore the correlation between rheologic performance and supramolecular structures of the polymer solutions.

EXPERIMENTAL

Reagents

AM was recrystallized twice from $CHCl_3$, and 2-acrylamido-2-methylpropane sulphonate (AMPS) from Lubrizol Company (Ohio, USA). PL with low molecular weight and butyl styrene were prepared in the laboratory.[11,12] HPAM (intrinsic viscosity: 30.14 dL^{-1} g) was purchased from DaQing Polymer Company (DaQing, China). Other reagents were analytically pure and used without further purification.

Instrumentation

The UV spectrum was obtained with a UV–240 spectrophotometer (Shimadzu Company, Shimane, Japan), and the polymer concentration in pure water was 0.1g dL^{-1}. The FT-IR spectrum was conducted in a NICOLET-560 FT-IR spectrophotometer with a resolution capacity of 1 cm^{-1}, and the scanning number was 32. The KBr disks were prepared with the purified polymer sample. The purified PASA and PASA-PL solutions in D_2O were measured with a 400 MHz Inova-400 instrument (Varian Company, California, USA) at the room temperature. The concentrations of the samples in D_2O were 10 mg mL^{-1}. The carbon, nitrogen, and hydrogen contents of the polymer were determined with a CARLO ESRA-1106 elemental analyzer (Italy). The molar percentage composition of the polymer was calculated from the measured elemental composition data. The intrinsic viscosities were measured with a 0.6 mm Ubbelohde capillary viscometer at $(30.0 \pm 0.1)°C$ in a 1.0 mol L^{-1} sodium nitrate solution. The apparent viscosities were measured by a Brookfield DVIII R27112E viscometer at a shear rate of 7.34 s^{-1} at 45°C. Fluorescence spectra were recorded on a Hitachi-7000 spectrophotofluorometer at 45°C, and the pyrene concentration in the polymer solutions was 3×10^{-5} mol L^{-1}. The SEM images were taken by an S-3000N SEM (Hitachi, Japan) with a resolution of 3 nm and a magnifying multiple of 3–300,000.

The steady shear and viscoelastic properties were investigated with a Gemini 200 dynamic rheometer (Malvern Instruments Company, England, UK) with cone-plate geometry (angle: 4° and diameter: 40 mm). The constant temperature was controlled at 45°C via a thermostatic system, and the accuracy degree was $\pm$ 0.1°C. During the dynamic measurement, the optimum strain was first determined, and the samples were measured for 8 min in the range of 0.08–50 rad s^{-1}. For the steady shear, the shear rate ranged from 0.1 to 300 s^{-1} and the measuring time of a shear cycle was 12 min. The measured data of steady shear were fitted according to the power law model:

$$\tau = K\gamma^n \quad \text{and} \quad \eta_{app} = \tau/\gamma = K\gamma^{n-1} \tag{1}$$

where τ is the shear stress, η_{app} is the apparent viscosity, γ is the shear rate, K is the consistency coefficient, and n is the power-law index.

Synthesis of PASA and PASA-PL

The PASA copolymer was synthesized by the free radical micellar copolymerization.[13] A 100-mL three-necked round flask was equipped with a mechanical stirrer, nitrogen inlet, and outlet. AM (5.0 g, 0.0704 mol), AMPS (1.6357 g, 0.007892 mol), and sodium dodecyl sulphate (SDS; 1.0105 g) were dissolved in 20.21 mL of distilled water and the solution was placed in the flask. NaOH was used to control the pH value of the reaction solution between 6 and 7. The mixture was stirred for 15 min, and BST (0.1010 g, 6.3139×10^{-4} mol) was then added into the reaction flask. The flask was purged with N_2 for half an
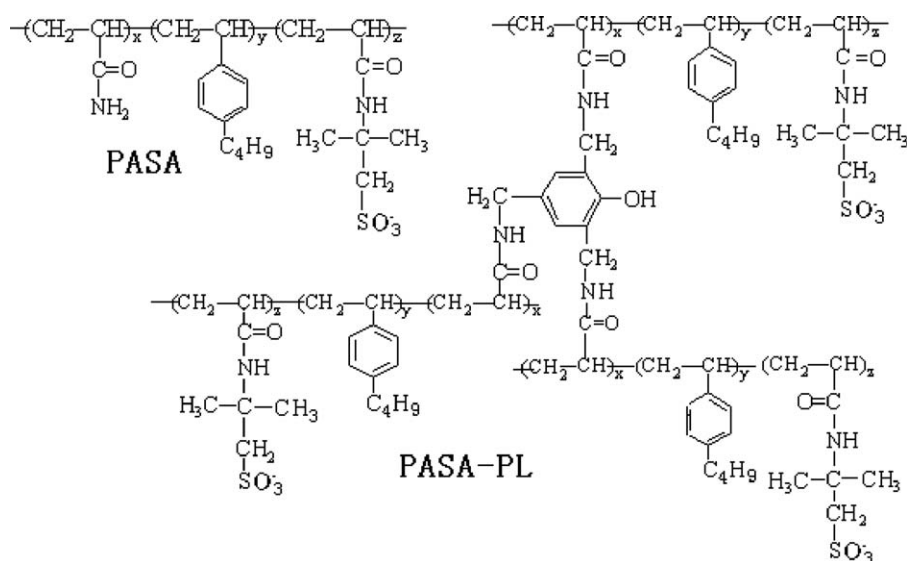
Figure 1 Schematic representation of molecular structures of PASA and PASA-PL.

hour. The reactant solution was heated to 50°C with stirring in a tempering kettle under nitrogen atmosphere, and 5.98 mL of 0.005 mol L^{-1} $K_2S_2O_8$ solution was then added into the reactant solution. After the polymerization proceeded for 16 h at 50°C, the reaction mixture was diluted with 500 mL of distilled water, and two volumes of acetone was then added with stirring to precipitate the polymers. The polymers were washed with acetone twice and extracted with ethanol by the Soxhlet extraction instrument for 2 days to remove surfactant and residual monomers. Finally, the polymers were dried in vacuo at 50°C for 3 days.

The main component of PL with low molecular weight is 2, 4, 6-trimethylolphenol. PL used as the crosslinking agent was added to the PASA or HPAM solutions, and the pH values of the mixtures were adjusted between 8 and 11. The concentration ratio of PASA to PL was 4 for all polymer solutions. The mixtures were placed in the color comparison tubes. After sealed with rubber stopples and medical rubberized fabric, the tubes were placed in the constant temperature oven. The crosslinking reaction proceeded for 3–4 days at 90°C to obtain the micro-crosslinked PASA-PL or HPAM–PL.

The molecular structures of PASA and PASA-PL are shown in Figure 1. The intrinsic viscosities of the PASA polymers with the BST feed amounts of 0.5 and 0.8 mol% are 7.81 and 6.72 dL^{-1} g, respectively. The molar compositions of the polymers (AM : NaAMPS : BST) are 88.19 : 11.24 : 0.57, and 88.33 : 10.65 : 1.02, respectively. There is a typic absorption peak at 230 nm attributed to the phenyl group for the UV spectrum of PASA. FT-IR peaks (cm^{-1}) of PASA are: —N—H stretch, 3433; C=O stretch, 1647; —CH$_3$, —CH$_2$, —CH stretch, 2863, 2928, 2787; —CH$_3$,

—CH$_2$, —CH bending, 1455, 1354, 1325; =C—H in phenyl stretch, 3090; —SO$_3^-$:1205, 1120, 1041, 634. Besides the above peaks of PASA, FT-IR peaks of PASA-PL (cm^{-1}) include —OH in PL stretch, 3206; —OH in PL bending, 1410; —C=C— in phenol stretch, 1612, 1560.

The ^{1}H NMR (400 MHz) shifts δ (ppm) of PASA are: 4H (—CH of phenyl), 7.028–7.787; 2H (—CH$_2$ of BST main chain), 2.105; 1H (—CH of BST main chain), 2.772; 6H (—CH$_3$ of NaAMPS side chain), 1.674; 2H (—CH$_2$ of AMPS side chain), 3.439; 2H (—CH$_2$ of NaAMPS main chain), 1.781; 1H (—CH of AMPS main chain), 2.355; 2H (—CH$_2$ of AM main chain), 1.500; 1H (—CH of AM main chain), 2.246; H (—NH$_2$ of AM side chain and —NH of AMPS side chain), 4.716–4.967.

RESULTS AND DISCUSSION

Influence of micro-crosslink on thickening properties

Figure 2(a,b) show the influence of polymer concentration on apparent viscosity for linear PASA and micro-crosslinked PASA-PL in 50 g L^{-1} NaCl solution, respectively. The solution viscosity increases sharply with increasing polymer concentration above 1.5 g L^{-1} for PASA, which indicates that C_p^* is 1.5 g L^{-1}. For the PASA-PL brine solution, an obvious increase in solution viscosity with increasing polymer concentration is exhibited above 0.7 g L^{-1} which is C_p^*. The result shows that the PASA polymer is micro-crosslinked with PL to result in an obvious decrease of C_p^* and a great increase in solution viscosities. The molecular weight of polymer and the rigidity of polymer chains are enhanced through
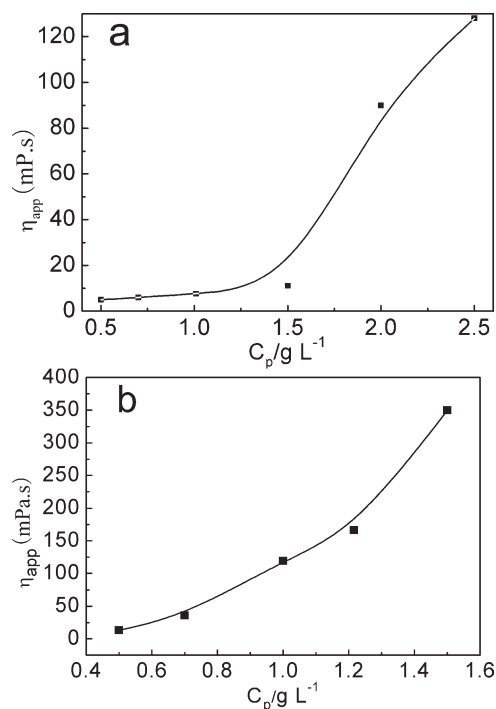
Figure 2 Influence of polymer concentration on apparent viscosity for PASA and PASA-PL in 50 g L^{-1} NaCl solutions. (a) PASA; (b) PASA-PL.

the micro-crosslink. Consequently, the intermolecular hydrophobic association and thickening effect of the polymer in brine solution are strengthened, leading to high solution viscosities at low polymer concentrations. This is demonstrated by the fluorescent probe investigation.

Figure 3(a,b) show the pyrene emission spectra of 1.5 g L^{-1} PASA and 1.5 g L^{-1} PASA-PL in 50 g L^{-1} NaCl solution, respectively. The intensity ratio I_1/I_3 of the first (375 nm) to the third (384 nm) vibronic peaks in the fluorescence emission spectrum is very sensitive to the nonpolarity of the local microenvironment of the pyrene probe. The lower the I_1/I_3 value is, the stronger the nonpolarity is. Thus, the formation of hydrophobic microdomains in aqueous and brine solutions can be determined by the I_1/I_3 value. Moreover, when the concentration of pyrene in a hydrophobic microenvironment is high enough for an excited pyrene (Py^*) and a pyrene in its ground state to come into close proximity during the Py^* lifetime, pyrene excimers are formed.[14] For hydrophobically associating polymers, the intensity ratio I_e/I_m of the pyrene excimer emission peak (about 475 nm) to monomer emission peak (399 nm) can characterize the association degree of hydrophobic groups in hydrophobic microdomains. The I_1/I_3 value of pyrene is 1.76 in pure water.[15] For 1.5 g L^{-1} PASA brine solution, the I_1/I_3 and I_e/I_m values are 1.128 and 1.524, respectively. By comparison, for 1.5 g L^{-1} PASA-PL brine solution, the I_1/I_3 value (0.848) is

lower than that in the PASA brine solution, and the I_e/I_m value (6.537) is much higher than that in the PASA brine solution. The results indicate that the micro-crosslink of PASA with PL leads to much stronger hydrophobic association and a remarkable increase of non-polarity of hydrophobic microdomains.

Steady shear properties of the PASA-PL brine solution

Figure 4(a) shows the influence of shear rate on the apparent viscosity upon consecutive three shear cycles for the PASA-PL brine solution with 1.2 g L^{-1} PASA, 0.30 PL g L^{-1}, and 50 g L^{-1} NaCl. During the first shear process with an increase in shear rate, the polymer brine solution exhibits shear thickening behavior at a very low shear rate, followed by a slow reduction in apparent viscosity. Then the solution viscosity increases remarkably with increasing shear rate from 10 to 30 s^{-1}, and finally decreases. The viscosities in the followed five shear measurements are obviously higher than that in this shear measurement below 10 s^{-1}. In the second shear reversion with a decrease in shear rate, the viscosity is also higher than that in the corresponding shear process below 30 s^{-1}. These results display shear thickening behavior of the PASA-PL brine solution.
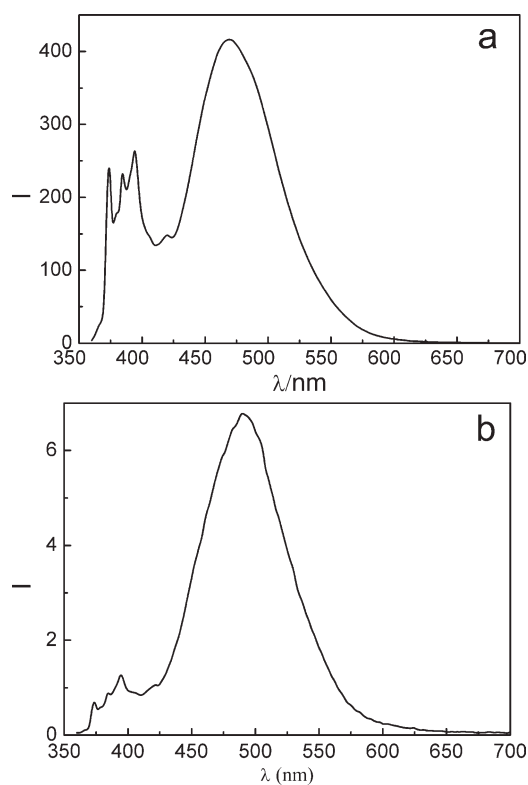

Figure 3 Fluorescence spectra of pyrene in PASA and PASA-PL brine solutions. Polymer concentration: 1.5 g L^{-1}, NaCl concentration: 50 g L^{-1}. (a) PASA brine solution; (b) PASA-PL brine solution.
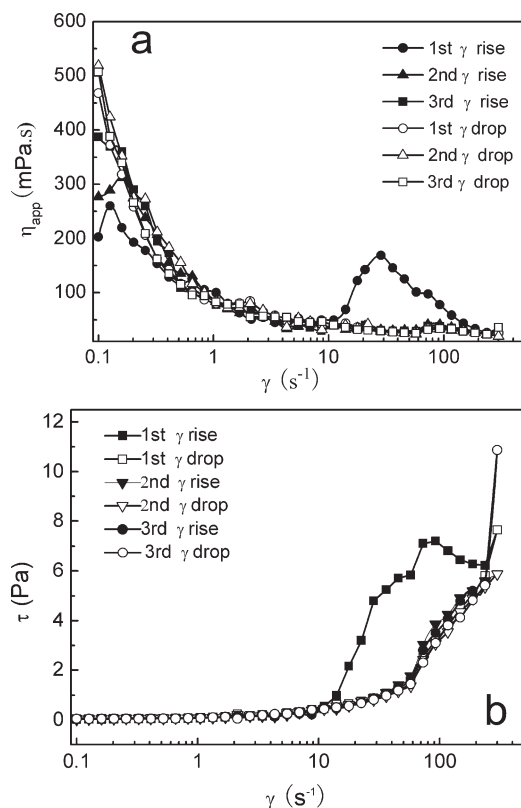
Figure 4 Influence of shear rate on apparent viscosity and shear stress upon three shear cycles for the PASA-PL brine solution with 1.2 g L^{-1} PASA, 0.30 g L^{-1} PL and 50 g L^{-1} NaCl. (a) Apparent viscosity; (b) shear stress.

The apparent viscosities of five shear processes are different slightly above 70 s^{-1}. Figure 4(b) displays the variation of shear stress with shear rate during three shear cycles for this brine solution. The shear stress is almost zero below 10 s^{-1} for every shear process. This suggests that the polymer chains are not expanded, but the sizes of aggregates vary at low shear rates. For the first shear, the shear stress rises abruptly with increasing shear rate above 10 s^{-1} and the polymer chains are expanded. The expansion is greatly favorable for the intermolecular hydrophobic association, resulting in the aforementioned increase in apparent viscosity. For the other five shear measurements, the slow variation of shear stress with shear rate in the range of 10–60 s^{-1} implies that the associated aggregates are disrupted and the polymer chains are gradually expanded. Finally, the molecular chains are greatly expanded and orientate in fluid field at a shear rate higher than 60 s^{-1}, resulting in a dramatic increase in shear stress.

The coiled polymer chains and compact aggregates are formed in the brine solution because of the charge shielding by Na^+ ions on $-SO_3^-$ groups along polymer chains. The proposed mechanism supported by the experimental results is as follows:

for the first shear process, some coiled polymer chains with weak intramolecular association become expanded upon shearing at a very low shear rate. The intermolecular association is reinforced and more associated aggregates are formed, resulting in an increase in apparent viscosity. Then large associated structures are gradually changed to form smaller aggregates with increasing shear rate. But the polymer chains are not deformed. With increasing shear rate from 10 to 30 s^{-1}, a large number of crosslinked polymer chains with strong intramolecular association are expanded, which greatly facilitates the intermolecular hydrophobic association. Moreover, compact aggregates become looser and possess larger hydrodynamics volume. Consequently, the brine solution exhibits an obvious shear thickening behavior. The intermolecular hydrophobic association is weakened upon shearing above 30 s^{-1}, the supramolecular structures are gradually disrupted, and the polymer chains are greatly expanded. This results in a low solution viscosity and high shear stress. The repetitious shear cycles show that the intermolecular hydrophobic association is reversible, and that the degradation of polymer chains does not occur upon shearing.

The shear behavior of the HPAM–PL brine solution was investigated to compare its solution performance with the associated PASA-PL brine solution. Figure 5(a) shows the influence of shear rate on the apparent viscosity upon consecutive three shear cycles for the HPAM–PL brine solution with 1.5 g L^{-1} HPAM and 50 g L^{-1} NaCl. During the first shear process, the brine solution exhibits shear thickening behavior at a shear rate lower than 1.13 s^{-1}, followed by an obvious decrease in apparent viscosity below 5 s^{-1}. Finally, the solution viscosity tends to be constant. For the first shear reversion, the viscosity is higher than the primary viscosity below 0.3 s^{-1}. The viscosities of the six shear measurements are almost the same above 10 s^{-1}, and the solution displays Newtonian fluid behavior. The viscosity of the third shear reversion is remarkably lower than those of the other five shear measurements through repetitive shear over the shear rate range, especially below 5 s^{-1}. The results show that the apparent viscosity of the HPAM–PL brine solution is not recovered after repetitive shear. This is different from the shear behavior of PASA-PL brine solution. The thickening ability of HPAM–PL depends on the super-high molecular weight and the entanglement of polymer chains. The coiled polymer chains become expanded through the first shear. The expansion can enhance the entanglement of polymer chains formed by the interaction of hydrogen bonds. Consequently, the shear thickening performance is exhibited. However, the polymer chains are disentangled after repetitive shear time after time, and the
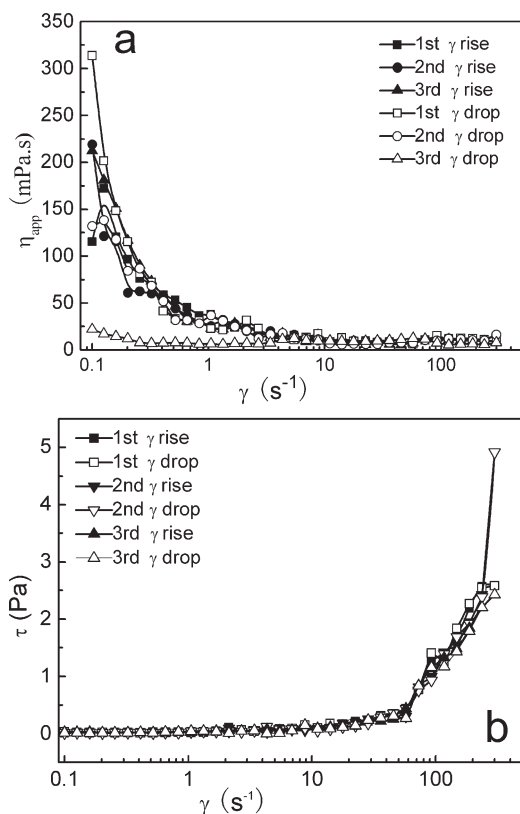
modulus (G') and viscous modulus (G'') are used to characterize viscoelastic properties. Moreover, the viscoelastic character of a polymer solution cannot be clearly determined from the values of G' and G'', but can be from the ratio G''/G' [tan δ (loss tangent)]. When tan δ is higher than 1, the polymer solution predominantly exhibits viscous behavior, contrariwise, the polymer solution predominantly exhibits elastic behavior. Figure 6(a,b) illustrate respectively G' and G'', and tan δ as a function of angular frequency for the PASA-PL and PASA aqueous solutions with a polymer concentration of 1.2 g L^{-1}. G' and G'' increase with an increase in angular frequency over the range of 0.08–50 rad s^{-1} for the two solutions. The PASA aqueous solution predominantly exhibits viscous behavior and G'' is remarkably higher than G' at an angular frequency lower than 3.0 rad s^{-1}. Then the solution predominantly exhibits elastic behavior, and the relaxation time is 0.34 s^{-1}. In addition, the tan δ value reduces sharply with increasing angular frequency from 0.3 to 3 rad s^{-1}, which indicates that the elastic character of the solution increases obviously. This is due to the transition of intramolecular hydrophobic association to intermolecular association at a suitable angular frequency. Whereas the PASA-PL aqueous
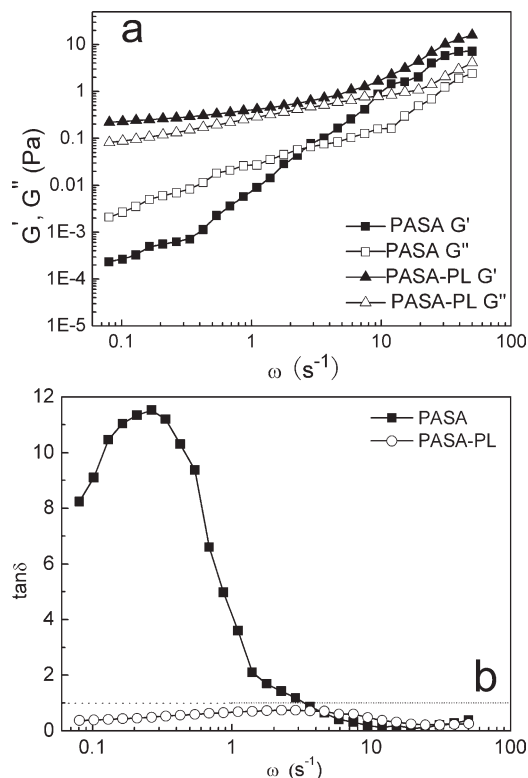
Figure 5 Influence of shear rate on apparent viscosity and shear stress upon three shear cycles for the HPAM-PL brine solution with 1.5 g L^{-1} HPAM, 0.30 g L^{-1} PL, and 50 g L^{-1} NaCl. (a) Apparent viscosity; (b) shear stress.

aggregated structures are disrupted. The entanglement of the HPAM–PL polymer chains can not be recovered completely after removing shear, resulting in an unrecovered solution viscosity. In addition, some molecular chains maybe degrade upon shearing at a high shear rate.

Figure 5(b) shows the plots of shear stress versus shear rate during three shear cycles for the aforementioned HPAM–PL brine solution. For six shear processes, the shear stress value of zero below 10 s^{-1} suggests that the polymer chains are not extended. The entanglement of polymer chains is merely disrupted, leading to the variation of sizes of aggregates at a low shear rate. As the shear rate increases from 10 to 60 s^{-1}, the shear stress increases slowly, and the polymer chains are gradually expanded. Finally, the shear stress rises abruptly at a shear rate higher than 60 s^{-1}, resulting in a great expansion of the molecular chains.

Effect of micro-crosslink on viscoelastic properties of PASA-PL brine solutions

The viscoelastic performance of PASA-PL and PASA solutions varies with angular frequency under the influence of a constant oscillatory strain. Elastic

Figure 6 Influence of angular frequency on elastic and viscous moduli, and loss tangent for the PASA-PL and PASA aqueous solutions. Polymer concentration: 1.2 g L^{-1}. (a) Elastic modulus G' and viscous modulus G''; (b) loss tangent tan δ.
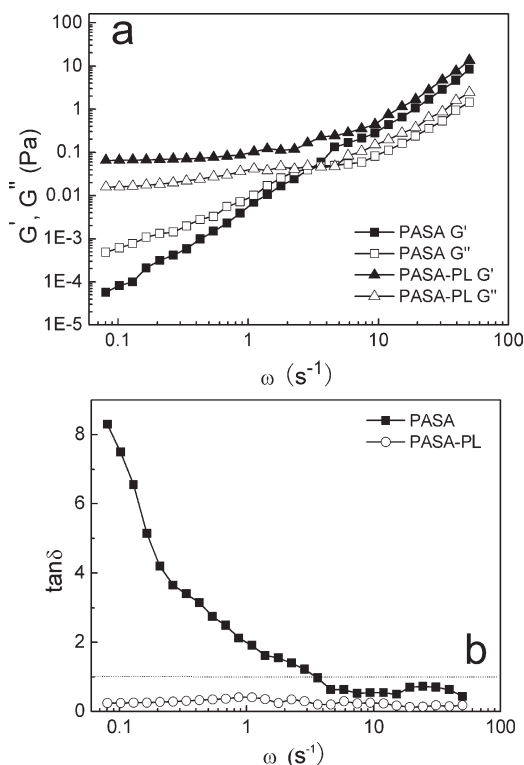
Figure 7 Influence of angular frequency on elastic and viscous moduli, and loss tangent of the PASA-PL and PASA brine solutions with 50.0 g L^{-1} NaCl. Polymer concentration: 1.2 g L^{-1}. (a) Elastic modulus G' and viscous modulus G''; (b) loss tangent tan δ.

solution predominantly exhibits elastic behavior and G' is remarkably higher than G'' over the whole angular frequency range. The results suggest that the micro-crosslink of PASA with PL can enhance remarkably the elastic character of the polymer solution because of the strengthened intermolecular hydrophobic association. This is resulted from an increase in molecular weight and rigidity of the polymer chains.

Figure 7(a,b) show respectively G' and G'', and tan δ as a function of angular frequency for the PASA-PL and PASA brine solutions with a polymer concentration of 1.2 g L^{-1} and 50 g L^{-1} NaCl. Both of the brine solutions exhibit respectively the similar variation of viscoelastic behavior with angular frequency to their aqueous solutions. However, G' and G'' of both brine solutions decrease remarkably in comparison with the corresponding aqueous solutions because of the weakened intermolecular hydrophobic association, which is due to the electrostatic shielding by Na$^+$ ions on —SO$_3$$^{-1}$groups along polymer chains. The tan δ value of the PASA brine solution reduces dramatically with increasing angular frequency over the angular frequency range because of the expansion of the coiled polymer chains and the formation of more associated structures upon suitable shearing.

Effect of polymer concentration on viscoelastic properties of PASA-PL solutions

Figure 8(a,b) show respectively G' and G'', and tan δ as a function of angular frequency for the PASA-PL brine solutions with 50 g L^{-1} NaCl at different polymer concentrations. G' and G'' increase with an increase in angular frequency over the range of 0.08–50 rad s^{-1} for all solutions, which indicates that these solutions exhibit more remarkable elastic deformation and viscous performance with increasing angular frequency. G'' is remarkably higher than G' at a low angular frequency for two PASA-PL brine solutions with 0.5 and 1.0 g L^{-1} PASA. As a result, the solutions predominantly exhibit viscous behavior, followed by elastic behavior above 2 rad s^{-1}. When the polymer concentrations are increased to 1.2 and 1.5 g L^{-1}, respectively, the polymer brine solutions predominantly exhibit elastic behavior over the whole angular frequency range, and the elastic characters remarkably enhance. A large number of coiled micro-crosslinked polymer chains are produced because of the strong intramolecular hydrophobic association at a polymer concentration lower than 1.0 g L^{-1}, and the weak intermolecular hydrophobic association results in the formation of small amounts of associated structures. However, as
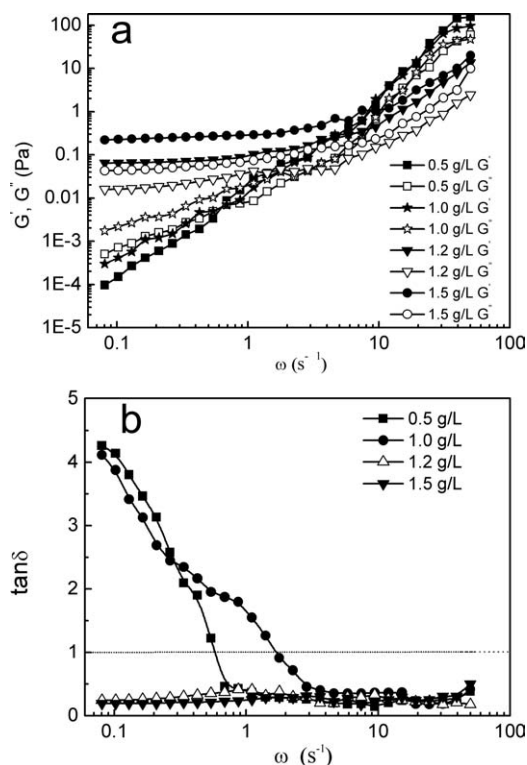

Figure 8 Influence of angular frequency on elastic and viscous moduli, and loss tangent of the PASA-PL brine solutions with different polymer concentrations. NaCl concentration: 50 g L^{-1}. (a) Elastic modulus G' and viscous modulus G''; (b) loss tangent tan δ.
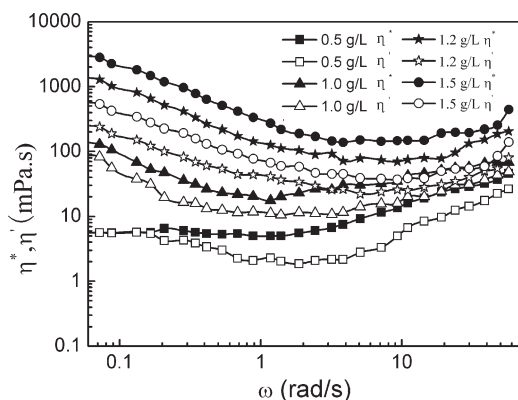
Figure 9 Influence of angular frequency on dynamic viscosity η' and complex viscosity η^* of the PASA-PL brine solutions with different polymer concentrations. NaCl concentration: 50 g L^{-1}.

angular frequency increases, the coiled polymer chains are expanded, and the intermolecular hydrophobic association is reinforced. Consequently, the elastic characters of the two brine solutions become more remarkable. The supramolecular structures predominantly exist in the PASA-PL brine solutions with the polymer concentration higher than 1.0 g L^{-1} because of the strong intermolecular hydrophobic association. When the polymer concentration is increased slightly from 1.2 to 1.5 g L^{-1}, G' and G'' of the PASA-PL brine solution increase obviously because of the formation of huge associated structures.[5]

The contribution of viscous and elastic character to the solution viscosity is expressed by dynamic viscosity (η') and elastic viscosity (η''), respectively, and the correlations of four parameters including G', G'', η', and η'' are given by

$$\eta'(\omega) = G''(\omega)/(\omega) \text{ and } \eta''(\omega) = G'(\omega)/\omega. \quad (2)$$

Complex viscosity (η^*) is used to characterize the viscoelastic behavior of a polymer solution and the total contribution of viscous and elastic character to the solution viscosity. The dependences of η' and η^* on angular frequency for the aforementioned four solutions are shown in Figure 9. η^* is equal to η' below 0.2 rad s^{-1}, and is then higher than η' at the polymer concentration of 0.5 g L^{-1}. This indicates that the hydrophobically associated structures have been formed at the polymer concentration. η^* is significantly higher than η' for the other three PASA-PL brine solutions over the angular frequency range. The strength of associated structures formed by the interaction of hydrophobic groups is restricted. Hence, some aggregates are destroyed by shear, and the complex and dynamic viscosities decrease with increasing angular frequency below 3 rad s^{-1} for the three brine solutions. The polymer chains are

extended above 10 rad s^{-1}, and accordingly the solution viscosities increase slightly.

Effect of NaCl concentration on viscoelastic properties of PASA-PL solutions

Figure 10(a,b) display respectively the variation of G' and G'', and tan δ with NaCl concentrations for the PASA-PL brine solutions with 1.2 g L^{-1} PASA. G' and G'' increase with an increase in angular frequency over the range of 0.08–50 rad s^{-1} for the four solutions, which indicates that the expanded molecular conformation is favorable for the presence of viscoelastic behavior of the brine solutions. The other three PASA-PL brine solutions predominantly exhibit elastic behavior over the whole range angular frequency except the 5 g L^{-1} NaCl solution. The elastic character of the 10 g L^{-1} NaCl solution is the most prominent, G' and G'' are at the maxima. The 5 g L^{-1} NaCl solution predominantly displays viscous behavior below 2 rad s^{-1}, followed by elastic behavior. For this solution, the polymer chains are coiled because of the charge shielding of the electrostatic repulsion, and by the addition of NaCl, the intramolecular association is strengthened and some aggregates are destroyed. This results in a loss of elastic
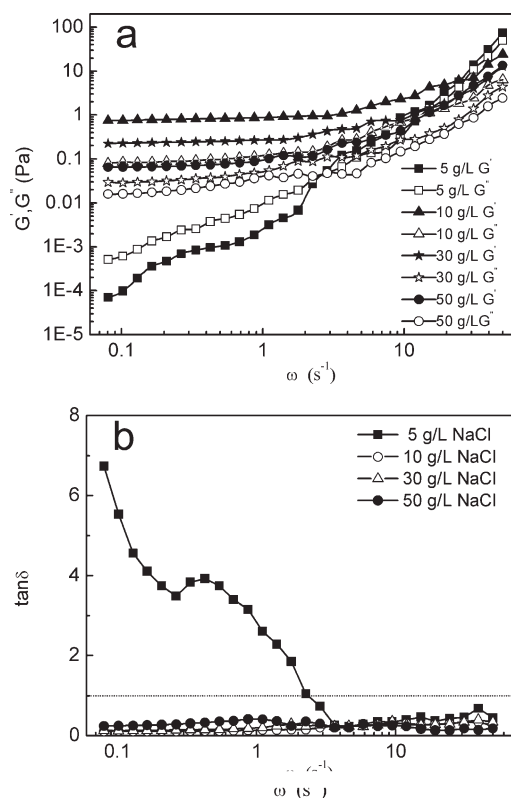

Figure 10 Influence of angular frequency on elastic and viscous moduli, and loss tangent of the PASA-PL brine solutions with different NaCl concentrations. Polymer concentration: 1.2 g L^{-1}. (a) Elastic modulus G' and viscous modulus G''; (b) loss tangent tan δ.
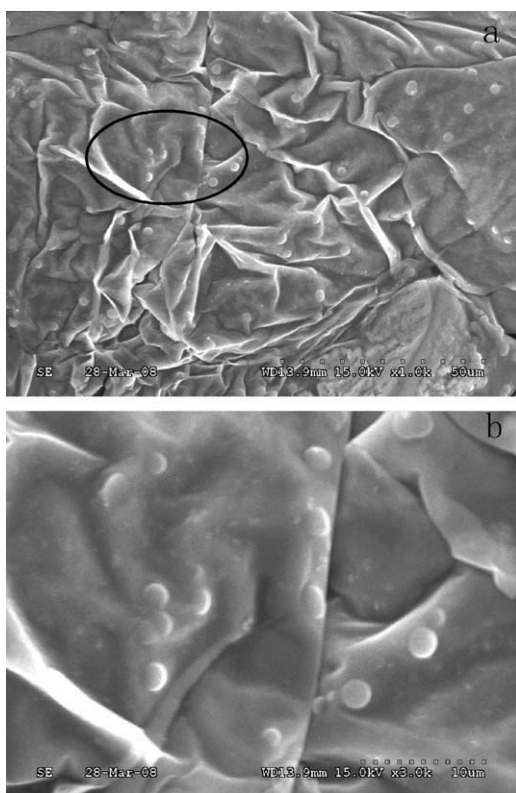
Figure 11 SEM images of 1.2 g L^{-1} PASA-PL in 10 g L^{-1} NaCl solution. (a) ×1000; (b) ×3000.

Figure 12 Influence of angular frequency on dynamic viscosity η′ and complex viscosity η* of the PASA-PL brine solutions with different NaCl concentrations. Polymer concentration: 1.2 g L^{-1}.

hydrophobically associated structures can lead to the significant viscoelastic performance in brine solutions.

Effect of BST feed amount on viscoelastic properties of PASA-PL brine solutions

Figure 13 displays the dependence of G′ and G″ on BST feed amount for the PASA-PL brine solutions with 1.2 g L^{-1} PASA and 50 g L^{-1} NaCl. G′ and G″ of the brine solutions increase obviously with increasing slightly BST feed amount from 0.5 to 0.8 mol%. When the BST feed amount is 0.5 mol%, G″ is remarkably higher than G′, and the brine solution predominantly displays viscous behavior below 2 rad s^{-1}. Then the micro-crosslinked polymer chains are extended and the brine solution exhibits an elastic character. For the PASA-PL brine solution with the BST feed amount of 0.8 mol%, G′ is remarkably higher than G″, and the brine solution predominantly exhibits elastic behavior over the whole angular frequency range. This shows that BST feed amount greatly influences the viscoelastic performance of the

and viscous character. However, with increasing NaCl concentration from 5 to 10 g L^{-1}, the charge shielding effect tends to reach the equilibrium, and the solution polarity induced by electrolytes increases. As a result, the intermolecular hydrophobic association is reinforced, leading to the enhanced viscoelastic properties. As NaCl concentration was further increased, the associated microstructures turn more compact, and G′ and G″ decrease. The continuous associated structures are formed in the 10 g L^{-1} NaCl solution (Fig. 11). These SEM images further demonstrate that the viscoelastic behavior of the PASA-PL brine solutions mainly depends on the strong intermolecular hydrophobic association.

Complex viscosities are higher than η′ over the whole angular frequency range for the aforementioned four brine solutions (Fig. 12). η* and η′ of the 10 g L^{-1} NaCl solution are at the maxima. The brine solutions display the remarkable salt-thickening effect in the range of 5–10 g L^{-1} NaCl. For the solutions of 10–50 g L^{-1} NaCl, as angular frequency increases, η* and η′ reduce below 10 rad s^{-1} because of the disassociation of aggregates, and then rise due to the expansion of polymer chains after shearing. η* and η′ are at the minima at 5 g L^{-1} NaCl, which is owing to the strongest charge shielding of repulsive interaction and the most disrupted associated structures. The results suggest that the excellent
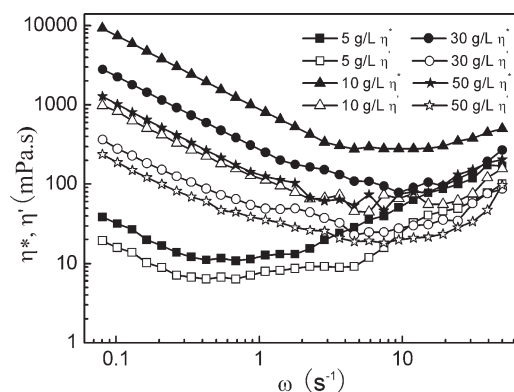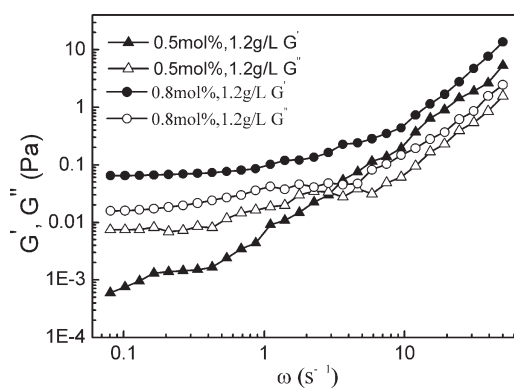

Figure 13 Influence of angular frequency on elastic modulus G′ and viscous modulus G″ of the PASA-PL brine solutions with different BST feed amount. Polymer concentration: 1.2 g L^{-1}.

PASA-PL brine solutions. The intermolecular hydrophobic association is weak at the low BST feed amount, and the viscoelastic behavior is mainly determined by the molecular weight of PASA-PL. When BST feed amount is slightly increased to 0.8 mol%, the micro-crosslink of PASA with PL can not only increase the molecular weight of polymer and enhance the rigidity of polymer chains, but also significantly strengthen the intermolecular hydrophobic association, leading to an obvious elastic character.

CONCLUSIONS

The steady shear and viscoelastic properties of brine solutions were investigated for the micro-crosslinked PASA-PL polymers with a hydrophobic monomer: butyl styrene. The micro-crosslink of the PASA polymer with PL can result in an obvious decrease of the critical associated concentration and a great increase in solution viscosities. For the PASA-PL brine solution with 1.2 g L^{-1} PASA and 50 g L^{-1} NaCl, the conformation of crosslinked polymer chains and the associated structures are remarkably influenced by shear rate upon steady shear for consecutive three cycles. The intermolecular hydrophobic association is greatly reinforced because of the expansion of the coiled PASA-PL chains at the suitable shear rate. As a result, more and larger associated aggregates are formed and the brine solution exhibits obvious shear thickening behavior. The supramolecular associated structures are gradually disrupted at a high shear rate, resulting in a low solution viscosity and high shear stress. The repetitious shear cycles show that the intermolecular hydrophobic association is reversible, and that the polymer chains do not degrade upon shearing. The HPAM–PL brine solution displays the different shear behavior from the PASA-PL brine solution. The thickening ability of HPAM–PL depends on the super-high molecular weight and the entanglement of polymer chains. The polymer chains are disentangled after repetitive shear time after time and maybe degrade at a high shear rate, resulting in an unrecovered apparent viscosity of the brine solution.

The micro-crosslink of PASA with PL can enhance remarkably the elastic character of the polymer aqueous and brine solutions because of the strengthened intermolecular hydrophobic association caused by the increase in molecular weight and rigidity of polymer chains. The increase in angular frequency is favorable for the elastic expansion of polymer chains for all PASA-PL aqueous and brine solutions. The PASA-PL brine solutions with 50 g L^{-1} NaCl predominantly exhibit elastic character over the angular frequency range at the polymer concentration higher than 1.0 g L^{-1}, which is remarkably strengthened with a slight increase in polymer concentration. The elastic performance of the PASA-PL brine solutions, with 0.5–1.5 g L^{-1} PASA, results in the complex viscosities significantly higher than the dynamic viscosities. The PASA-PL brine solutions with 1.2 g L^{-1} PASA display a salt-thickening effect and predominantly exhibit elastic character over the angular frequency range at 10–50 g L^{-1} NaCl. A slight increase in BST feed amount enhances obviously elastic character of the PASA-PL brine solution. These results demonstrate that the viscoelastic behavior of the PASA-PL solutions mainly depends on the formation of associated structures via the strong intermolecular hydrophobic association.

References

1. Grattoni, C. A.; Al-Sharji, H. H.; Yang C. H.; Muggeridge, A. H.; Zimmerman, R. W. J Colloid Interface Sci 2001, 240, 601.
2. Albonico, P.; Lockhart, T. P. ACS, Polym Prepr, Div Polym Chem 1991, 32, 610.
3. Cai, W. S.; Huang, R. H. Eur Polym J 2001, 37, 1553.
4. Zhong, C. R.; Huang, R. H.; Zhang, X.; Dai, H. J App Polym Sci 2007, 103, 4027.
5. Zhong, C. R.; Luo, T. T.; Deng, J. Polym Bull 2009, 103, 709.
6. Xia, H. F.; Wang, D. M.; Liu, Z. C.; Yang, Q. Y. Acta Petrolei Sinica (Chinese) 2001, 22, 60.
7. Wang, G.; Wang, D. M.; Xia, H. F.; Zhang, L. J. J Daqing Petroleum Institute (Chinese) 2007, 31, 25.
8. Camail, M.; Margaillan, A.; Martin, I. Polym Int 2009, 58, 155.
9. Yang, Q. B.; Song, C. L.; Chen, Q.; Zhang, P. P.; Wang, P. X. J Polym Sci Part B: Polym Phys 2008, 46, 2465.
10. Zhu, Z. Y.; Jian, O. Y.; Paillet, S.; Desbrieres, J.; Grassl, B. Eur Polym J 2007, 43, 824.
11. Qian, X. L.; Wu, W. H.; Yu, P. Z.; W, J. Q.; Li, X. Y.; Sun, Y. L. Oilfield Chem (Chinese) 2005, 22, 241.
12. Littke, A. F.; Schwarz, L. F.; Gregory, C. J. J Am Chem Soc 2002, 124, 6343.
13. Hill, A.; Candau, F.; Selb, J. Macromolecules 1993, 26, 4521.
14. Winnik, F. M. Chem Rev 1993, 93, 587.
15. Zhong, C. R.; Ye, L; Dai, H.; Huang, R. H. J Appl Polym Sci 2007, 103, 277.